



# ESR investigation of gamma irradiated sulbactam sodium

Sevgi Yurus\*, Turan Ozbey, Mustafa Korkmaz

*Physics Engineering Department, Hacettepe University, Beytepe, 06800 Ankara, Turkey*

Received 29 January 2004; received in revised form 18 March 2004; accepted 24 March 2004

Available online 9 June 2004

## Abstract

In the present work, radiolysis of gamma irradiated sulbactam sodium (SS) was investigated through detailed ESR studies performed at low and at high temperatures on the radiolytic products induced in this drug after gamma irradiation in the dose range of 3–15 kGy. While unirradiated SS presented no ESR signal, irradiated SS exhibited an ESR spectrum with many resonance peaks. Variations of the spectrum pattern and of the intensities of resonance peaks with microwave power, applied radiation dose, storage time and temperature were followed. A radical with unpaired electron localised on the carbon atom of five membered ring directly attached to two CH<sub>3</sub> groups and SO<sub>2</sub><sup>-</sup> ionic radical called as species A and B, respectively, were found to be produced after gamma radiolysis of SS. The characteristic spectral and kinetic features of these species were determined by spectrum simulation calculation and by curve fitting techniques using experimental signal intensity data as input. Although, species A was fairly unstable at room and especially at high temperatures, species B were observed to be relatively stable even at high temperatures having activation energies of  $E_A = 46(\pm 4)$  kJ/mol and  $E_B = 82(\pm 3)$  kJ/mol, respectively, at room temperature. Four different mathematical functions were tried to explore the dosimetric features of SS and a linear function of applied dose described best the dose–response data obtained for stable species, that is, radical B, in the dose range of 0–10 kGy. An accuracy of 4% in the dose measurements was concluded to be achievable through back-projection dose calculations if SS were used as a dosimetric material.

© 2004 Elsevier B.V. All rights reserved.

*Keywords:* Sulbactam sodium; Radiolysis; Radical; Dosimetry; ESR

## 1. Introduction

Sulbactam sodium (SS) is a derivative of the basic penicillin nucleus. Although, it alone possesses little useful antibacterial activity except against the Neisseriaceal, whole organism studies have shown that sulbactam restores ampicillin activity against

beta-lactamase producing strains. In particular, sulbactam has good inhibitory activity against clinically important plasmid mediated beta-lactamases, most frequently responsible from transferred drug resistance. Sulbactam has been shown to have no effect on activity of ampicillin against ampicillin susceptible strains. Thus, SS is used in combination with ampicillin sodium to protect it from the effect of a destructive enzyme (beta-lactamase) and to broaden the antibiotic spectrum of ampicillin to those bacteria normally resistant to it.

\* Corresponding author. Tel.: +90-312-297-72-13;

fax: +90-312-299-20-37.

*E-mail address:* [syurus@hacettepe.edu.tr](mailto:syurus@hacettepe.edu.tr) (S. Yurus).

The feasibility of sterilising semi-synthetic antibiotics belonging to the penicillin group by gamma radiation has been the subject of many earlier studies [1–6]. Accentuated susceptibility to hydrolysis of beta-lactam antibiotics at elevated temperature obviates their sterilisation by conventional methods prompting an interest in their sterilisation by radiation. However, sensitivity of the drug to radiation is an important parameter in this respect. To our knowledge, radiolysis of gamma irradiated SS is not investigated in the literature up to date. Thus, the aim of the present work is: to explore the radiolysis of gamma irradiated SS and to determine the dosimetric potential of SS through a detailed ESR investigation performed at room and at elevated temperatures on the characteristic features of the radiolytic products induced in SS after gamma irradiation.

## 2. Experimental

### 2.1. Materials

Sulbactam sodium of pharmaceutical grade was kindly supplied by Mustafa Nevzat Drug Company (İstanbul) and it was used as it was received without any further treatment. ESR investigation was principally performed on SS of pharmaceutical grade. Some experiments were also carried out on SS of spectroscopic grade, but no pattern changes were observed in the ESR spectra recorded at low and at high temperatures. Chemically, SS is sodium penicillinate sulfone; sodium (2S, 5R)-3,3-dimethyl-7-oxo-4-thia-1-azabicyclo (3,2,0) heptane-2-carboxylate 4,4-dioxide. The molecular structure of it is presented in Fig. 1.

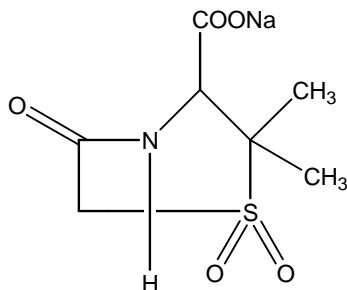


Fig. 1. Molecular structure of sulbactam sodium.

### 2.2. Irradiation

Irradiations were performed at room (290 K) or at 77 K using a  $^{60}\text{Co}$  gamma cell 220 as ionising radiation source (dose rate 2 kGy/h) in the dose range of 3–15 kGy. Sealed glass veils containing of about 2 g SS were irradiated at room temperature and the actual doses received by samples were determined by a Fricke dosimeter. The samples irradiated at 77 K were sealed in air, before radiation treatment in ESR quartz tubes, however, for room temperature study ESR tubes were sealed after treatment. A special care was paid to avoid the water condensation in the ESR tubes especially at low temperatures. A sealed unirradiated sample was kept as reference.

### 2.3. Instrumentation

ESR measurements were performed using a BRUKER EMX 131 X-band spectrometer equipped with a cylindrical cavity. Temperatures of samples inside the microwave cavity were monitored with a digital temperature control system (BRUKER ER 4111-VT). The latter gives opportunity of measuring the temperatures with an accuracy of  $\pm 0.5$  K at the site of sample. The evolutions of the ESR signal with the applied microwave power; received radiation dose, storage time and temperature were followed by calculating the signal area determined by double integration of derivative ESR spectra. A DPPH sample was used as standard.

A set of four different samples irradiated at a dose of 10 kGy were annealed at four different temperatures for predetermined times, and the data obtained were used to calculate the decay characteristics of radicals contributing to the ESR spectra of gamma irradiated SS, then activation energies of the involved radical species were calculated from Arrhenius plot.

### 2.4. Data analysis

Parameter values were calculated as the means of five different measurements carried out on five different samples prepared from the same SS batch irradiated at a given radiation dose. Analyses of experimental data were performed by adopting a model based on two radicals of different characteristic features. Numerical spectrum simulation calculations

were carried out using Win EPR software supplied by Bruker Company. Four different mathematical functions were tried to analyse applied dose–response data.

### 3. Results and discussion

While unirradiated SS samples exhibit no resonance signal, samples irradiated at room (290 K) and 77 K were observed to present ESR spectra with many resonance peaks as shown in Fig. 2a and b. Peaks of weak intensities were observed not appearing at low radiation doses even in samples irradiated at 77 K. Variations of the spectrum pattern and of the intensities of the assigned resonance peaks with microwave power, applied radiation dose, storage time and temperature were studied first, using spectra of the samples irradiated at room temperature.

#### 3.1. Samples irradiated at room temperature

##### 3.1.1. Variation of the signal intensities with microwave power

Variations of the intensities of the weak (1–7, 11–18) and strong peaks (8–10) with microwave power were studied first. Although, weak peaks start to saturate at very low microwave powers, strong peaks do not saturate even at 20 mW and they increase rather linearly up to relatively high powers (0–9 mW). Some weak peaks, such as 6, 7, 11 and 12 influenced in large extent, from the presence of strong peaks seems to saturate differently than the weak peaks not affected from the presence of strong peaks. The differences in the variations of the signal intensities and saturation behaviours of weak and strong peaks clearly imply that two different radical species are involved in the formation of the experimental ESR spectra of gamma irradiated SS and that the radical species dominating resonance peaks 8–10 saturates at higher microwave power. The results of the microwave saturation studies indicate that, although, peaks 7 and 11 belong to weak peaks, their intensities increase much faster than the other weak peaks but much slower than the intensities of strong peaks. This shows that weak peaks appearing just at the left and right sides of the strong central peaks (8–10) are affected heavily from the presence of the strong peaks.

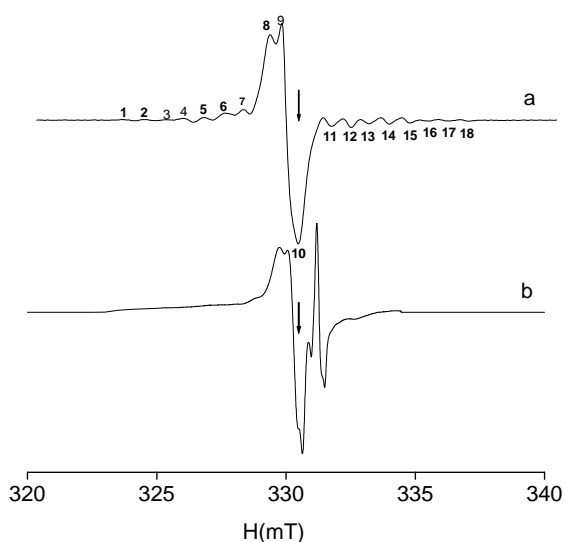


Fig. 2. ESR spectra of sulbactam sodium irradiated at room (290 K) and at 77 K at the doses of 10 and 1.2 kGy, respectively. Figures on room temperature spectrum indicate the numbers assigned to the observed resonance peaks. (a) 290 K and (b) spectra of a sample irradiated at 77 K and recorded at 110 K. Arrows on the spectra indicate the position of DPPH resonance line.

##### 3.1.2. Variation of the signal intensity with temperature

A variable temperature study was performed using samples irradiated at a dose of 10 kGy. Samples were first cooled down to 100 K starting from room temperature (290 K) with an increment of 20 K. Then, temperature was increased up to 410 K with the same increment. Spectra were recorded 5 min after setting the temperature. The results obtained for weak and strong peaks indicated that, although, all weak and strong peaks experience important increases when the temperature is decreased, they exhibit rapid irreversible decreases above room temperature originating from fast radical decays at these temperatures.

##### 3.1.3. The decay of the signal intensity in long term

Samples irradiated at a dose of 1.2 kGy were stored at room temperature open to air. The evolution of ESR spectra was observed over a period of 800 h by recording spectra in regular time interval without changing the positions of the samples in the microwave cavity during the storage period. Weak peaks which are extended over a large magnetic field range were observed to decay very fast with the same decay rate disappearing almost completely in a storage period

of about 180 h irrelevant from the irradiation dose. As for strong peaks, they exhibit significant increases while weak peaks decay, and then they start to decay with a very small decay constant over the storage period of 800 h. Experimental signal intensity decay data of weak and strong peaks were fitted to the exponentially decreasing functions, assuming that radical species responsible from weak and strong peaks obey to first order kinetics. Calculated decay constants by this technique for contributing radicals were found to be  $k$  (weak peaks) = 0.01190 ( $\pm 0.00080$ ) per hour and  $k'$  (strong peaks) = 0.00012 ( $\pm 0.00003$ ) per hour. From the decay curves obtained using calculated decay constants, it was concluded that exponentially decaying function describes fairly well experimental decay data relevant to weak and strong peaks and that radical species responsible from weak peaks are very unstable compared to the species responsible from strong peaks at room temperature under normal conditions. The increases observed in the intensities of strong peaks at the beginning of storage period (0–180 h) likely arise from fast decay of weak peaks contributing negatively to the strong peaks.

### 3.2. Samples irradiated at 77 K

Spectra of samples sealed in air before irradiation and irradiated at 77 K were also recorded at low (100 K) and at room temperature. A 100 K spectra of the samples irradiated at 77 K consisted of many other resonance peaks beside peaks appearing at the same magnetic field values like the strong peaks (assigned as 8–10) of the samples irradiated at room temperature did (Fig. 2b). Comparison of the spectra recorded at 100 K for empty and SS containing sample tubes irradiated at 77 K under the same conditions indicated that all other peaks except those having similar  $g$  values with those called for strong peaks, originate from the radical species induced in the quartz sample tubes. Although, strong peaks seen in the samples irradiated at room temperature appeared as well in the samples irradiated at 77 K, the weak peaks were interestingly absent.

#### 3.2.1. Variation of the signal intensity with microwave power

Saturation behaviours of the observed peaks originating from SS irradiated at 77 K were also studied

using the spectra recorded at 100 K of the samples. As is expected, saturation behaviours of the resonance peaks assigned as 8–10 at 100 K were very different from those obtained at room temperature for the same peaks. From the results of low temperature saturation study, it was concluded that all peaks exhibit the behaviour of a homogeneously broadened resonance line in the microwave power range of 0–10 mW and they start to saturate at a power level of as low as 0.1 mW. Heating the samples irradiated at 77 K up to room temperature (290 K) was observed not producing any pattern changes in the ESR spectra of gamma irradiated SS. However, observed resonance lines were found displaying the microwave saturation behaviours of strong peaks of samples irradiated at room temperature.

### 3.3. Kinetic features of the radical species at high temperatures

The decays of the free radicals are expected to depend on the temperature. That is, an increase in the temperature is supposed to bring about faster decays of the radicals. To test this idea and to calculate the activation energies of the radicals responsible from ESR spectra of gamma irradiated SS, kinetic behaviours of the radicals at four different temperatures were studied. SS irradiated at room temperature at a dose of 10 kGy is divided into four equal parts and transferred to ESR tubes, and then they are annealed at temperatures 313, 343, 353, and 363 K for 60 min. Spectra were recorded at a step of 10 min at the annealing temperatures. Variations of the peak intensities versus annealing time were plotted. The results obtained for strong peak 10 originating from radical called as species B are given in Fig. 3 as an example of these variations. It was difficult to perform a reliable annealing study basing on the data obtained through the intensity measurements of not completely resolved low and high field resonance peaks arising from radical of relatively low concentration called as species A. It was rather due to the overlap of the central peaks of both radical species involved in the formation of ESR spectra and to fairly unstable character of the species A even at room temperature. Although, strong peaks are quite stable up to 330 K, they start to decay relatively fast above this temperature about up to 365 K then they begin to increase (not given in the present work).

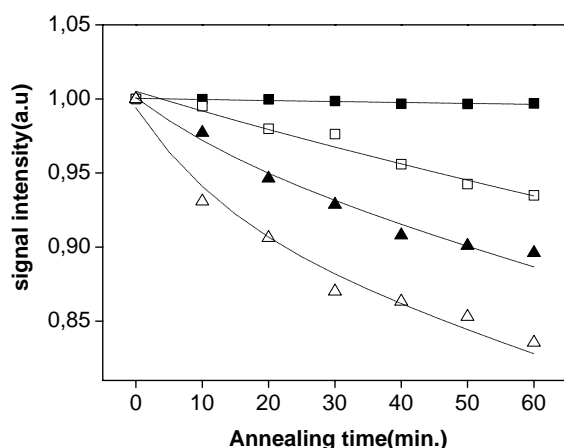


Fig. 3. Effects of annealing temperature and time on signal intensities of strong peak 10. Symbols: experimental (■) 313 (□) 343 (▲) 353 and (△) 363 K, respectively; solid lines: theoretical.

It is seen that the decreases in the signal intensities become faster with the increase in annealing temperature, that is, the higher the temperature the faster the decay. The increases observed in the intensities of all strong peaks above about 365 K likely originate from thermal creation of the radical species of same or similar spectroscopic features to those created by gamma radiation. Thermal creation rate of the radical species responsible from strong peaks was very weak or zero at low temperature so that the decay process dominates thermal behaviours of the signal intensities of peaks 8–10. However, the increase in temperature incites the increase in thermal creation rate of these species. Thus, the decay and creation process both start to dominate thermal behaviours with comparable weights and at

nearly 400 K the rates of these two competitive processes become almost equal. Calculated experimental signal intensity decay data at each annealing temperature for strong peaks, were fitted to a function being the sum of two exponentially decreasing functions associated with species A and B assuming that they obey first order kinetics in the temperature range of 313–363 K. The results obtained for decay constants are summarised in the Table 1. It is seen that, radical A decay much faster than the radical B and that theoretical decay data (Fig. 3) calculated using the decay constants given in Table 1 are in good agreement with experimental results. Activation energies of radical species A and B were also calculated using the decay constants given in Table 1 and the following values were obtained for species involved in the formation of ESR spectra of irradiated SS ( $E_A = 46(\pm 4)$  kJ/mol,  $E_B = 82(\pm 3)$  kJ/mol). In accordance with the decay in long term at room temperature, the activation energy of radical species A which decays faster is relatively small compared with that of species B decaying slowly.

#### 3.4. Simulation calculations and proposed tentative radical species

In accordance with the results obtained from microwave and high temperature kinetic studies, a model predicting the presence of two radical species having rhombic and isotropic  $g$  tensors and without and with hyperfine structure, respectively, was tried to simulate room temperature ESR spectrum of a sample irradiated at a dose of 10 kGy. Parameters calculated by this technique for contributing radical species and

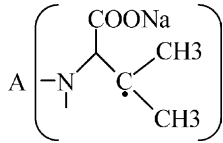
Table 1  
Calculated decay constants for contributing radicals using the data derived from high temperature annealing studies

Annealing temperature (K)	Radical species	Decay constant ( $\text{min}^{-1}$ ) $10^5$	Correlation coefficient
313	A	679 ( $\pm 119$ )	0.753
	B	3 ( $\pm 1$ )	
343	A	3180 ( $\pm 1301$ )	0.977
	B	108 ( $\pm 6$ )	
353	A	5873 ( $\pm 1276$ )	0.982
	B	148 ( $\pm 6$ )	
363	A	7129 ( $\pm 821$ )	0.977
	B	182 ( $\pm 12$ )	

Figures in parentheses are the estimated error on the relevant parameters.

Table 2

Spectroscopic parameters calculated by spectrum simulation for contributing radical species

Radical species	Spectroscopic parameters				
	$g_{xx}$	$g_{yy}$	$g_{zz}$	$A_H$ (mT)	$A_N$ (mT)
A 	2.0028	2.0028	2.0028	2.250	0.824
B [SO <sub>2</sub> <sup>-</sup> ]	2.0022	2.0054	2.0097	–	–

theoretical spectra obtained using these parameters are given in Table 2 and in Fig. 4, respectively. Calculated rhombic  $g$  values correlate well with both experimental  $g$  values determined in the present work for strong resonance peaks: 8 ( $g_8 = 2.0082$ ); 9 ( $g_9 = 2.0057$ ); 10 ( $g_{10} = 2.0022$ ) and with those reported in the literature for SO<sub>2</sub><sup>-</sup> ionic radical induced in sulphur containing compounds irradiated by gamma radiation [7–14]. In fact, SO<sub>2</sub> is the most sensitive sub group to radiation in SS molecule due to its high electrophilic feature, and is expected to be at the origin of the observed three strong resonance lines dominating ESR spectra through the formation of SO<sub>2</sub><sup>-</sup> ionic radical species that is called radical B in the present work. Excluding SO<sub>2</sub> group from SS molecule gives rise to

the generation of another radical species (called radical A) with unpaired electron localised on the carbon atom bound directly to two CH<sub>3</sub> groups. The unpaired electron of radical A interacts with only five protons of CH<sub>3</sub> groups and with the nucleus of nitrogen atom present on the five-member ring. One of the CH<sub>3</sub> protons likely is not involved in the formation of hyperfine structure due to the specific spatial orientation of one of the C–H bond that the proton makes with the carbon atom carrying the unpaired electron.

### 3.5. Dosimetric feature of SS

Beside qualitative detection, the ESR spectroscopy can also be used for dose estimation. However, critical point in this respect is the choice of mathematical function(s) used to describe the dose–response curve,

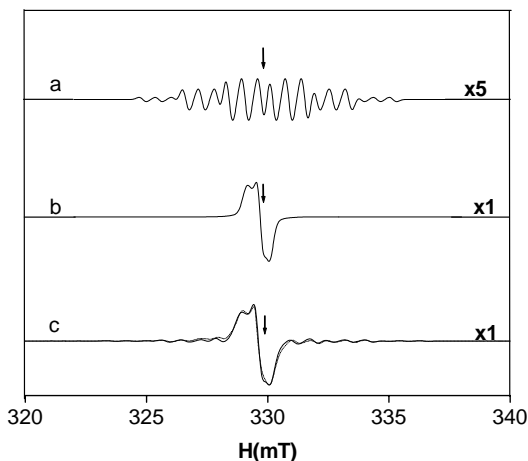


Fig. 4. Experimental and calculated spectra for gamma irradiated SS. (a) spectrum of radical A (b) that of radical B (c) experimental (dotted line) and calculated sum (full line) spectra. Arrows indicate the position of DPPH signal.

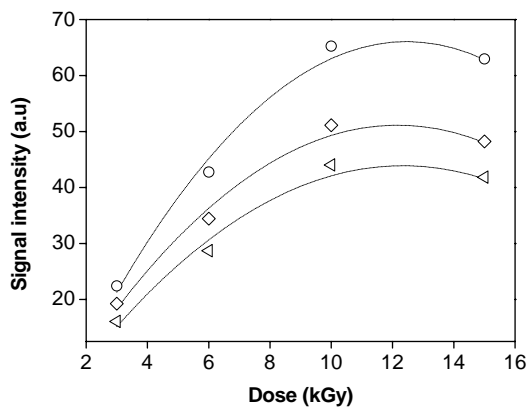


Fig. 5. Variation of signal intensities with applied radiation dose. Symbols: experimental ( $\triangle$  (8)  $\diamond$  (9)  $\circ$  (10)); dotted lines: theoretical results obtained by fitting experimental data to a function comprising a linear and a quadratic dose terms.

Table 3

Functions tried to describe experimental dose–response data obtained for strong peaks and parameter values calculated by curve fitting techniques

Function	Resonance peak	Parameters	Correlation coefficient
$I = k + ID$ (linear)	8	$I = 4.36(\pm 0.72) + 3.99(\pm 0.10) D$	0.9997
	9	$I = 6.20(\pm 1.74) + 4.53(\pm 0.28) D$	0.9985
	10	$I = 4.90(\pm 2.28) + 6.09(\pm 0.33) D$	0.9986
$I = n + mD + pD^2$ (linear + quadratic)	8	$I = -6.30(\pm 0.81) + 8.14(\pm 0.39) D - 0.33(\pm 0.03) D^2$	0.9843
	9	$I = -6.58(\pm 0.77) + 9.49(\pm 0.37) D - 0.39(\pm 0.03) D^2$	0.9889
	10	$I = -11.56(\pm 0.98) + 12.46(\pm 0.47) D - 0.50(\pm 0.04) D^2$	0.9974
$I = rD^g$ (power)	8	$I = 10.97(\pm 0.82) D^{0.53(\pm 0.03)}$	0.8459
	9	$I = 13.55(\pm 1.00) D^{0.50(\pm 0.03)}$	0.8363
	10	$I = 15.38(\pm 1.12) D^{0.56(\pm 0.03)}$	0.8546
$I = s[1 - \exp(-dD)]$ (exponential)	8	$I = 4.97(\pm 2.65)[1 - \exp(-0.15(\pm 0.018)D)]$	0.9202
	9	$I = 56.33(\pm 2.90)[1 - \exp(-0.164(\pm 0.020)D)]$	0.9202
	10	$I = 76.03(\pm 4.07)[1 - \exp(-0.143(\pm 0.016)D)]$	0.9251

Figures in parentheses are the estimated error on the relevant parameters.

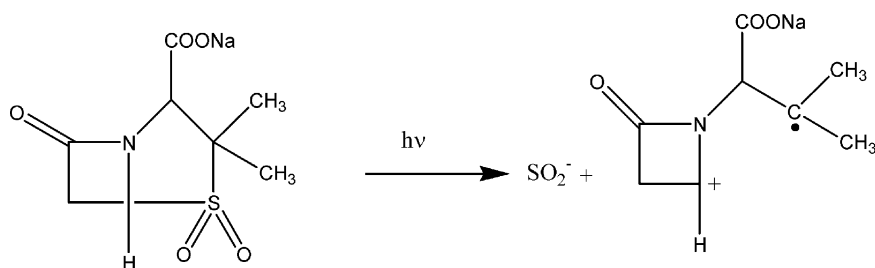
that is, signal intensity calculated by double integration technique versus applied dose curves. Strong peaks (8–10) only, arising from species B, were considered in the evaluation of dosimetric feature of gamma irradiated SS due to its high radiation yield toward species B in the dose range of (0–10 kGy) more suitable for radiation dose measurements. The results obtained concerning the variation of signal intensity with applied dose are given in Fig. 5. Signal intensity data in the dose range of 0–10 kGy were related to the absorbed dose ( $D$ ) in kGy through four different functions given in Table 3. These functions have been mentioned previously in different works for estimation of the absorbed dose in the radiation processed food [15,16] and irradiated pharmaceuticals [17,18]. Parameter values calculated through fitting experimental dose–response data to the equations given in the Table 3 are also presented in the same table. It should be noted that no attempt has been made to force the curves to pass through origin. Interestingly, in the dose range of 1–10 kGy, a linear function of applied dose was found to correlate reasonably well with the experimental data obtained for resonance peaks 8–10, although this correlation was much better for peaks 8 than the peaks 9 and 10.

The utility of the equation describing best the experimental dose–response data, that is, the linear equation, was tested by calculating the interpolated doses. To do this, experimental signal intensities obtained

for strong peaks were entered into the equation and corresponding doses ( $D_c$ ) were calculated. The results were presented as the ratio of the difference between calculated ( $D_c$ ) and measured ( $D_m$ ) doses to measured doses. These data indicated that with a proper calibration, SS could be used as a good dosimetric material and that gamma radiation dose could be measured with accuracy better than 4% in the dose range of 0–10 kGy.

#### 4. Conclusion

Although unirradiated SS exhibits no ESR signal, gamma irradiated SS presents an ESR signal consisting of many resonance peaks. However, the intensities of these peaks are very different suggesting the presence of two radical species of different weight and spectroscopic features in gamma irradiated SS. Microwave saturation, kinetic studies at room and at high temperatures and detailed spectrum simulation calculations indicated that, in fact, a radical species with rhombic g tensor presenting no hyperfine structure and a second one with isotropic g tensor and with hyperfine structure are responsible from ESR spectrum of gamma irradiated SS. Radiolysis of SS molecule in accordance with reaction given below was thought to be responsible from the production of these radical species.



The exclusion of  $\text{SO}_2$  group from molecular structure of SS gives rise to the formation of a  $\text{SO}_2^-$  ionic radical (radical B) and a second radical (radical A) having unpaired electron localised on the carbon atom bound directly to two  $\text{CH}_3$  groups. Spectroscopic parameters determined from spectrum simulation calculations for proposed tentative radical species were found to correlate well with those reported in the literature for similar radicals [8–14,19–21]. Radical species A and B are relatively stable at room temperature, however, species B has a higher activation energy ( $E_B = 82(\pm 3)$  kJ/mol) than the species A ( $E_A = 46(\pm 4)$  kJ/mol). The presence of ESR signal originating from radical B even after 90 days of storage was considered as an indication of distinguishing irradiated SS from unirradiated one.

A linear function of applied dose described best experimental dose–response data among other three mathematical functions tried in the present work. Radiation yield of gamma irradiated SS toward radical B is very high compared to that for radical A. Back-projection calculation showed that SS presents the properties of a good dosimetric materials and that radiation dose can be measured with an accuracy of 4% in the dose range of 0–10 kGy based on the resonance peaks originating from radical B.

## References

- [1] G.P. Jacobs, *Int. J. Appl. Radiat. Isot.* 30 (1979) 417–421.
- [2] G.P. Jacobs, *Int. J. Pharm.* 4 (1980) 299–307.
- [3] G.P. Jacobs, *Drug Dev. Ind. Pharm.* 6 (1980) 547–552.
- [4] G.P. Jacobs, *Int. J. Appl. Radiat. Isot.* 35 (1984) 1023–1027.
- [5] M. Gibella, A.S. Crucq, B. Tilquin, P. Stocker, G. Lesgards, J. Raffi, *Radiat. Phys. Chem.* 58 (2000) 69–76.
- [6] C. Schüttler, K.W. Bögl, *J. Radiat. Steril.* 1 (1994) 327–345.
- [7] M.I. Samoilovich, L.I. Tsinober, *Sov. Phys. Crystallogr.* 14 (1970) 656–666.
- [8] L.V. Bershov, V.O. Martirosyan, A.S. Marfunin, A.V. Speranskii, *Fortschr. Miner.* 52 (1975) 591–604.
- [9] R. Huzimura, *Jpn. J. Appl. Phys.* 18 (1979) 2031–2032.
- [10] O. Katzenberger, R. Debuyst, P. De Canniere, F. Dejehet, D. Apers, M. Barabas, *Appl. Radiat. Isot.* 40 (1989) 1113–1118.
- [11] M. Barabas, A. Bach, R. Mudelsee, A. Mangini, *Q. Sci. Rev.* 11 (1992) 165–171.
- [12] A. Kai, T. Miki, *Radiat. Phys. Chem.* 40 (1992) 469–476.
- [13] R. Walther, M. Barabas, A. Mangini, *Q. Sci. Rev.* 11 (1992) 191–196.
- [14] Ş. Çolak, M. Korkmaz, *Int. J. Pharm.* 267 (2003) 49–58.
- [15] M.E. Desrosiers, G.L. Wilson, C.R. Hunter, *Appl. Radiat. Isot.* 42 (1991) 613–616.
- [16] M.E. Desrosiers, *Appl. Radiat. Isot.* 42 (1991) 617–619.
- [17] J.P. Basly, I. Basly, M. Bernard, *J. Pharm. Biomed. Anal.* 17 (1998) 871–875.
- [18] J.P. Basly, I. Longy, M. Bernard, *Anal. Chim. Acta* 359 (1998) 107–113.
- [19] C. Corvaja, H. Fisher, G. Giacometti, *Z. Physik. Chem. Neue Folge* 45 (1965) 1–8.
- [20] P.B. Ayscough, C. Thomson, *Trans. Faraday Soc.* 58 (1962) 1477–1484.
- [21] R.W. Fessenden, R.H. Schuler, *J. Chem. Phys.* 39 (1963) 2147–2152.